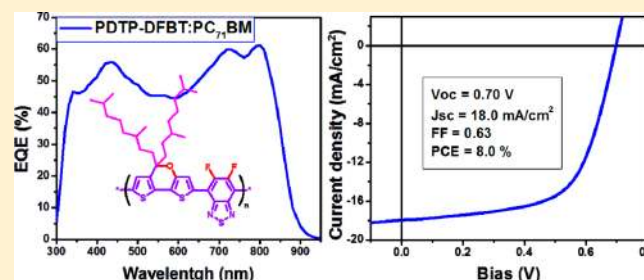


Synthesis of 5*H*-Dithieno[3,2-*b*:2',3'-*d*]pyran as an Electron-Rich Building Block for Donor–Acceptor Type Low-Bandgap PolymersLetian Dou,<sup>†,‡</sup> Chun-Chao Chen,<sup>†</sup> Ken Yoshimura,<sup>\*,§</sup> Kenichiro Ohya,<sup>§</sup> Wei-Hsuan Chang,<sup>†,‡</sup> Jing Gao,<sup>†</sup> Yongsheng Liu,<sup>†</sup> Eric Richard,<sup>†</sup> and Yang Yang<sup>\*,†,‡</sup><sup>†</sup>Department of Materials Science and Engineering and <sup>‡</sup>California NanoSystems Institute, University of California, Los Angeles, Los Angeles, California 90095, United States<sup>§</sup>Tsukuba Material Development Laboratory, Sumitomo Chemical Co., Ltd., 5-15, Kitahama, Higashi-ku, Osaka, 541, Japan

## S Supporting Information

**ABSTRACT:** We describe the detailed synthesis and characterization of an electron-rich building block, dithienopyran (DTP), and its application as a donor unit in low-bandgap conjugated polymers. The electron-donating property of the DTP unit was found to be the strongest among the most frequently used donor units such as benzodithiophene (BDT) or cyclopentadithiophene (CPDT) units. When the DTP unit was polymerized with the strongly electron-deficient difluorobenzothiadiazole (DFBT) unit, a regiorandom polymer (PDTP–DFBT, bandgap = 1.38 eV) was obtained. For comparison with the DTP unit, polymers containing alternating benzodithiophene (BDT) or cyclopentadithiophene (CPDT) units and the DFBT unit were synthesized (PBDT–DFBT and PCPDT–DFBT). We found that the DTP based polymer PDTP–DFBT shows significantly improved solubility and processability compared to the BDT or CPDT based polymers. Consequently, very high molecular weight and soluble PDTP–DFBT can be obtained with less bulky side chains. Interestingly, PDTP–DFBT shows excellent performance in bulk-heterojunction solar cells with power conversion efficiencies reaching 8.0%, which is significantly higher than PBDT–DFBT and PCPDT–DFBT based devices. This study demonstrates that DTP is a promising building block for high-performance solar cell materials.



## ■ INTRODUCTION

Organic photovoltaic (OPV) devices provide a promising way to utilize the solar energy efficiently while maintaining low cost.<sup>1</sup> The design and synthesis of low-bandgap (LBG) conjugated polymers for use as electron donor materials for bulk heterojunction (BHJ) polymer solar cell (PSC) applications have attracted remarkable attention during the past decade.<sup>2</sup> So far, power conversion efficiencies (PCEs) of 7–8% for single junction and 9–10% for tandem devices have been achieved using carefully designed polymers as p-type materials and fullerene derivatives (for example, [6,6]-phenyl-C<sub>71</sub>-butyric acid methyl ester [PC<sub>71</sub>BM]) as n-type materials.<sup>3,4</sup> A small energy bandgap of the polymers is usually obtained by using the “donor–acceptor” strategy to construct the backbone.<sup>2</sup> Proper alignment of the highest occupied molecular orbital (HOMO) and lowest unoccupied molecular orbital (LUMO) energy levels can be achieved by tuning the relative strength of the electron-rich unit and electron-deficient unit.<sup>2</sup> Good charge transport properties can be attained by using building blocks with large  $\pi$ -conjugation and good planarity, enhancing the molecular weights, fine-tuning the solubilizing side chains, etc.<sup>2</sup> A large number of electron donor units have been synthesized, for example, the carbazole (Cz), benzodithiophene (BDT), dithienosilole/dithienogermole (DTS/DTG), and cyclopentadithiophene (CPDT) units.<sup>5–8</sup> By combining these donor units

with different electron acceptor units such as thienopyrroldione (TPD), diketopyrrolopyrrole (DPP), or thienothiophene (TT), several conjugated polymers with excellent photovoltaic performance have been reported.<sup>5–8</sup> Notably, these units have been developed for several years and are relatively well-studied. Therefore, a nonconventional molecular design of new building blocks for the donor–acceptor polymers with high photovoltaic performance should be interesting to the field.

Very recently, we demonstrated a tandem PSC with National Renewable Energy Laboratory certified efficiency of 10.6%, incorporating a new LBG polymer, PDTP–DFBT. The polymer is based on an asymmetric electron-donating unit and an electron-withdrawing difluorobenzothiadiazole (DFBT) unit.<sup>4c</sup> However, the detailed synthesis and characterization of this unique structure have never been reported. Herein, we describe the synthesis and characterization of the electron-rich building block 5*H*-dithieno[3,2-*b*:2',3'-*d*]pyran (DTP) and its application in high performance photovoltaic polymers. The chemical structures of the conventional BDT, CPDT, and the newly designed DTP units are shown in Figure 1. To examine the photovoltaic performance of the new DTP unit, a series of

Received: March 1, 2013

Revised: April 12, 2013

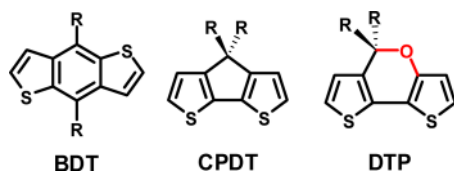


**Figure 1.** Chemical structures of BDT, CPDT, and DTP units. R = alkyl chains (for example, 3,7-dimethyloctyl is used in this study).

LBG polymers based on alternating BDT or CPDT or DTP unit and DFBT unit were synthesized (PBDT–DFBT, PCPDT–DFBT, and PDTP–DFBT). Compared to the polymers based on BDT and CPDT units, the DTP based polymer shows lower bandgap, better solubility, enhanced charge carrier mobility, and more favorable thin film morphology. Interestingly, BHJ solar cell devices based on PDTP–DFBT show PCE as high as 8.0% with photoresponse up to 900 nm, which is significantly higher than BDT and

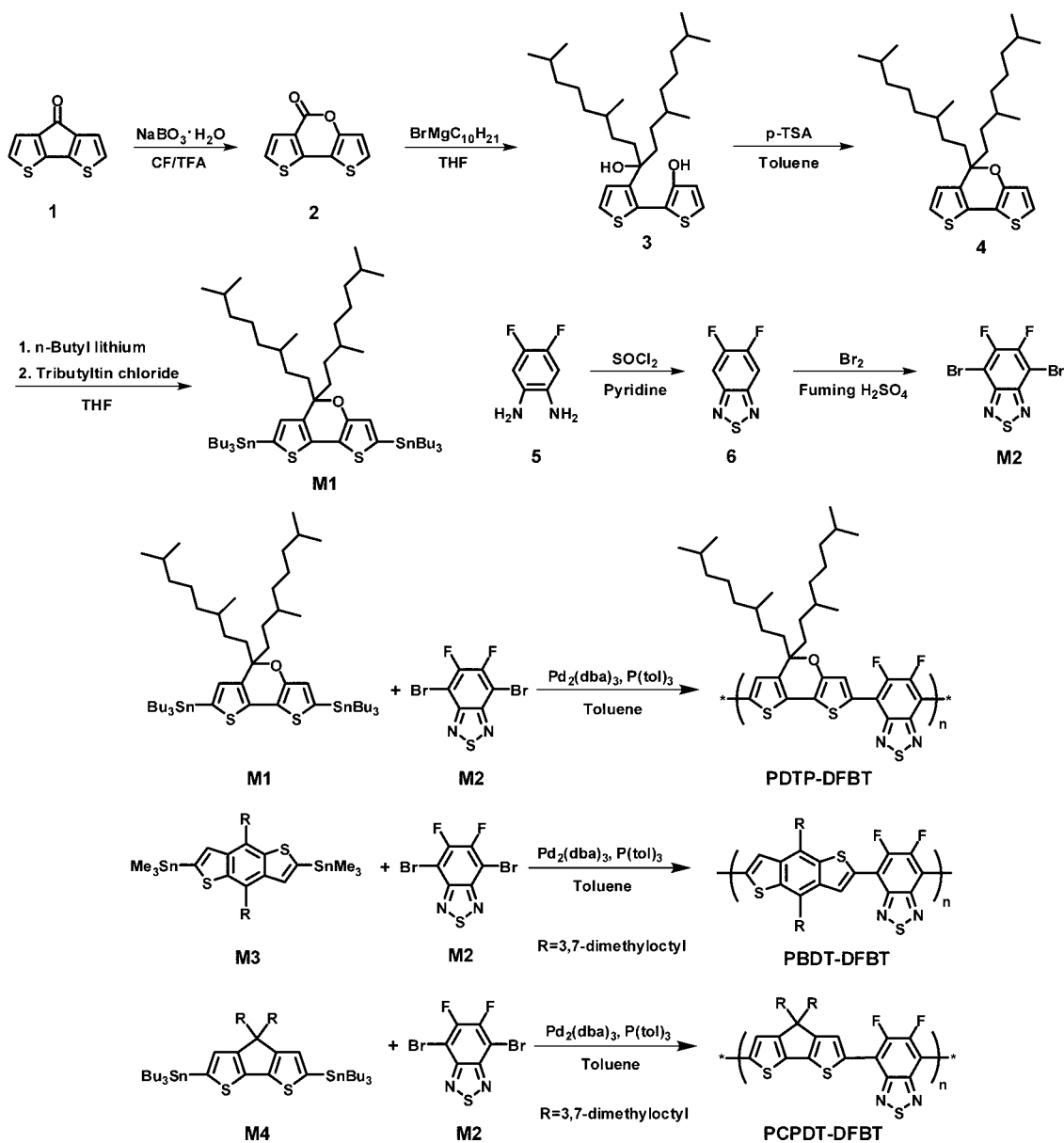
CPDT based polymers. The high photovoltaic performance can be attributed to the following reasons: (1) the strong electron-donating property of the DTP unit results in a very small energy gap of the DFBT-co-polymer, allowing it to absorb more photons in the NIR region; (2) due to the significantly improved solubility of the DTP based polymers, less bulky side chains can be used to achieve very high molecular weight polymers with good charge transport properties and thin film morphology.

## EXPERIMENTAL SECTION

**Materials Synthesis.** The synthetic routes of the DTP unit and the polymers are shown in Scheme 1.

**Reagents.** 4*H*-Cyclopenta[2,1-*b*:3,4-*b'*]dithiophene-4-one (compound 1) was purchased from SunaTech Inc. (Rubipy Scientific Inc.). 3,4-Difluoro-1,2-diaminobenzene (compound 5) was purchased from Matrix Scientific Inc. [6,6]-Phenyl-C<sub>71</sub>-butyric acid methyl ester (PC<sub>71</sub>BM) was purchased from Nano-C. Unless otherwise stated, all of the other chemicals were purchased from Aldrich and used as received.

**Scheme 1.** Synthetic Routes of M1, M2, PDTP–DFBT, PBDT–DFBT, and PCPDT–DFBT



**Compound 2.** In a 250 mL round-bottom flask, compound 1 (5 g, 27 mmol) was dissolved in 50 mL of chloroform and 50 mL of trifluoroacetic acid. Sodium perborate monohydrate (6.4 g, 63 mmol) was added into the solution in one portion, and the mixture was stirred at room temperature (25 °C) for 45 min. Then, 200 mL of water and 200 mL of chloroform were added to extract the organic part. The solvent was removed by an evaporator. The compound was purified by silica gel chromatography using a dichloromethane (DCM) and hexane mixture (1:1, v:v) as the eluent to obtain a white solid (1.6 g, yield 30%). <sup>1</sup>H NMR (CDCl<sub>3</sub>, 400 MHz): 7.66 (d, 1H), 7.47 (d, 1H), 7.27 (d, 1H), 7.11 (d, 1H).

**Compound 3.** In a 100 mL two-neck round-bottom flask, compound 2 (1.2 g, 5.7 mmol) was dissolved in 30 mL of dehydrotetrahydrofuran (THF) under argon protection. The flask was kept at −20 °C; 12.7 mL of 1 M diethyl ether solution of 3,7-dimethyloctylmagnesium bromide was added slowly. Then, the temperature was raised to room temperature and kept stirring for 6 h. The reaction was stopped by adding 20 mL of water into the solution, and the organic part was extracted by ethyl acetate. The ethyl acetate solution was dehydrated with sodium sulfate. The solution was then passed through a silica gel column, and the solvent was removed. 2.8 g of compound 3 was obtained as light yellow oil (yield 90%). <sup>1</sup>H NMR (CDCl<sub>3</sub>, 400 MHz): 8.42 (br, 1H), 7.27 (d, 1H), 7.21 (d, 1H), 6.98 (d, 1H), 6.74 (d, 1H), 2.74 (br, 1H), 1.92 (m, 4H), 1.55–1.00 (br, 20H), 0.92 (s, 6H), 0.89 (s, 12H).

**Compound 4.** In a 100 mL two-neck round-bottom flask, compound 3 (1.5 g, 3.0 mmol) was dissolved in toluene (30 mL) in a flask under argon protection. 100 mg of sodium *p*-toluenesulfonic acid monohydrate was added into the solution and stirred for 1.5 h at 110 °C. The solution was cooled down to room temperature, and 50 mL of water and 30 mL of toluene were added to extract the organic part. The toluene solution was dried with sodium sulfate, and then the solvent was removed. The compound was purified by silica gel chromatography using hexane as the eluent to obtain a yellow oil (1.3 g, yield 95%). <sup>1</sup>H NMR (CDCl<sub>3</sub>, 400 MHz): 6.98 (d, 1H), 6.93 (d, 1H), 6.68 (d, 1H), 6.60 (d, 1H), 1.90 (m, 4H), 1.54–1.01 (br, 20H), 0.89 (s, 6H), 0.85 (s, 12H) (Figure S1).

**Compound M1.** In a 100 mL two-neck round-bottom flask, compound 4 (0.58 g, 1.2 mmol) was dissolved in THF (20 mL) in a flask under argon protection. Keep the solution at −78 °C. 1.7 mL (2.7 mmol) of *n*-butyllithium was dropped into the solution slowly. The solution was stirred at −78 °C for 30 min and room temperature for 2 h. Then 0.92 mL of tributyltin chloride (3.4 mmol) was added at −78 °C in one portion. Stirring was maintained at room temperature for 6 h, and then 30 mL of water was added to quench the reaction. 30 mL of hexane was added to extract the organic part, and the solvent was removed under vacuum. The product was purified by silica gel column with hexane as eluent. (In advance, the silica gel was dipped into hexane contains 10% triethylamine for 1 h and flushed out with hexane.) After removing the solvent, M1 was obtained as brownish oil (1.18 g, yield 92%). <sup>1</sup>H NMR (CDCl<sub>3</sub>, 400 MHz): 6.71 (d, 1H), 6.68 (d, 1H), 1.96–1.80 (br, 4H), 1.64–1.00 (br, 56H), 0.89–0.82 (m, 36H) (Figure S2).

**Compound 6.** In a 500 mL two neck round-bottom flask, compound 5 (6.0 g, 41.7 mmol) was dissolved in 60 mL of pyridine in a flask under argon protection. 6.2 mL (85.4 mmol) of thionyl chloride was added in 20 min at 0 °C. The mixture was stirred at room temperature for 6 h. 200 mL of water and 200 mL of DCM were added to extract the product. The organic part was washed with water 2–3 times to remove pyridine. The solvent was removed under vacuum, and the product was purified by silica gel chromatography using a hexane and ethyl acetate mixture (4:1, v:v) as the eluent to obtain a white solid (3.3 g, yield 46%). <sup>1</sup>H NMR (CDCl<sub>3</sub>, 400 MHz): 7.75 (t, 2H). <sup>19</sup>F NMR (CDCl<sub>3</sub>, 400 MHz): −128.3 (s, 2F). GC-MS: 172.0 [M<sup>+</sup>] (purity >98%).

**Compound M2.** In a 100 mL two neck round-bottom flask, compound 6 (2.5 g, 14.5 mmol) was dissolved in fuming sulfuric acid (30 mL) in a flask under nitrogen protection. 7 mL of bromine was added into the flask in one portion. The mixture was stirred at 60 °C for 24 h. The mixture was cooled down and then poured it into 500

mL of ice–water to afford a large amount of white precipitate. The precipitate was filtered and collected and then purified by silica gel chromatography using a hexane and ethyl acetate mixture (4:1, v:v) as the eluent to obtain a white solid. The white solid was recrystallized in methanol to afford a white needle-like crystal (1.9 g, yield 40%). <sup>19</sup>F NMR (CDCl<sub>3</sub>, 400 MHz): −118.9 (s, 2F). GC-MS: 330.0 [M<sup>+</sup>] (purity >99%).

**Polymerization for PDTP–DFBT.** M1 (0.431g, 0.410 mmol) and M2 (0.131g, 0.397 mmol) were dissolved into 20 mL of toluene in a flask protected by argon. The solution was flushed with argon for 10 min, and then 7 mg of Pd<sub>2</sub>(dba)<sub>3</sub> and 14 mg of P(*o*-tol)<sub>3</sub> were added into the flask. The solution was flushed with argon again for another 10 min. The oil bath was heated to 100 °C gradually, and the reaction mixture was stirred for 4 h at 100 °C under an argon atmosphere. 400 mg of bromobenzene was added, and the mixture was stirred for 4 h. Then, the mixture was cooled down to room temperature, and the polymer was precipitated in 100 mL of methanol and the precipitated solid was collected. Low molecular weight portion was removed by Soxhlet extraction using acetone (6 h) and hexane (12 h). The polymer which remained in the extraction thimble was dissolved into 50 mL of chlorobenzene, to which was added 2 g of sodium diethyldithiocarbamate and 40 mL of water followed by stirring at 80 °C for 6 h. The aqueous phase was removed, and the organic phase was washed with 50 mL of water twice and then with 50 mL of 3 wt % acetic acid aqueous solution twice, followed by two more washings with 5% potassium fluoride aqueous solution and two more washings with water. The polymer was further purified by silica gel chromatography using chlorobenzene as eluent. Then the polymer was precipitated in 100 mL of methanol and obtained as dark purple solid; yield ~70%. The polymer can be dissolved chlorobenzene or dichlorobenzene, etc. <sup>1</sup>H NMR (400 MHz, CDCl<sub>3</sub>): *d* = 6.8–7.8 (br, 2H), 0.6–2.0 (br, 42H). *M<sub>n</sub>* = 28.5 kDa (Figure S3); polydispersity = 2.2. PBTD–DFBT and PCPDT–DFBT were synthesized using the same procedure but much shorter polymerization time (~20 min).

**Materials Characterization, Device Fabrication, and Measurements.** See Supporting Information for the details.

## RESULTS AND DISCUSSION

**Material Design and Synthesis.** The synthetic routes of DTP, DFBT, and related polymers are shown in Scheme 1. The detailed synthesis procedure is described in the Experimental Section.<sup>9</sup> Monomers M3 and M4 were synthesized using reported methods.<sup>6a,8b</sup> First, compound 2 was obtained via Baeyer–Villiger oxidation by sodium perborate monohydrate from compound 1 at room temperature with yield ~30%.<sup>10</sup> The low yield of this step is possibly due to the oxidation of other positions on compound 1. Then, compound 2 was treated with excess Grignard reagent at room temperature to yield compound 3 with 90% yield. The solubilizing side chain, 3,7-dimethyloctyl (DMO), can be incorporated onto the DTP unit. Next, the ring-closing reaction was carried out by adding sodium *p*-toluenesulfonic acid (*p*-TSA) into a toluene solution of compound 3 and refluxing for 1–2 h. The DTP compound (compound 4) was purified by silica gel chromatography 2–3 times using hexane as the eluent and was obtained as a yellow oil with high yield. Monomer M1 was made using the conventional method: (1) Lithiation by *n*-butyllithium at low temperature and (2) addition of tin compound (typically trimethyltin chloride) to the mixture to form the ditin monomer. However, the tin compounds are usually difficult to purify by silica gel chromatography due to their poor stability.<sup>3d</sup> Here, we chose tributyltin instead of trimethyltin to increase the stability to the silica gel, and also, we treated the silica gel with triethylamine before use to passivate the weak acidity. By doing these, very pure compound M1 can be obtained by passing through a deactivated silica gel column



(NMR is shown in Supporting Information Figures S1 and S2). The DFBT unit was synthesized using a method similar to the reported ones, but with some modification.<sup>11</sup> For the first step, using pyridine instead of triethylamine as the solvent can enhance the yield from ~20% to ~50%. Then, monomer **M2** was attained by bromination using liquid bromine and fuming sulfuric acid at 60 °C for 24 h. It was found that other milder conditions for making the DFBT monomer (such as bromine/HBr, bromine/Fe, etc.) led to 5–10% monobromo product, which is very difficult to separate. By using the method reported here, less than 1% monobromo product was detected by gas chromatography–mass spectroscopy (GC-MS) analysis.

PDTP–DFBT was polymerized via Stille-coupling polymerization using  $\text{Pd}_2(\text{dba})_3/\text{P}(o\text{-tol})_3$  as catalyst in toluene and obtained as a purple solid. It should be pointed out that the purification of this polymer is more complicated than our previously reported high performance polymers.<sup>3a,4a,b</sup> In previous work, trimethyltin was used for making the monomer, and the remaining end group could be easily removed by passing through a silica gel column. The tributyltin group used here is more stable to silica gel and cannot be removed completely by a silica gel column. To solve this problem, bromobenzene was used to end-cap the polymers, and the polymers were washed with 3% acetic acid and 5% potassium fluoride aqueous (see Supporting Information for more details). Elemental analysis using X-ray fluorescence (XRF) of the polymers reveals that the remaining tin can be reduced from ~0.12% to <0.05%. The photovoltaic performance of PDTP–DFBT with and without tin removal will be examined in this work. The gel permeation chromatography (GPC) measurements show average molecular weights ranging from 9.7 to 28.5 kDa for different batches. The polymer is thermally stable up to 340 °C as indicated by thermogravimetric analysis (TGA) (see Figure S4 for TGA results). For comparison, PBDT–CPDT and PCPDT–DFBT with the same DMO side chains are also synthesized using the same method. However, both of them show poor solubility in common solvents, especially for PBDT–DFBT. Because of the extremely low solubility of PBDT–DFBT, no further characterization was carried out on it. The solubility issue of the polymers will be discussed in this article.

**Solubility Issue of the Polymers.** It is well-known that achieving high molecular weight is critical for excellent photovoltaic performance, since it will facilitate the bicontinuous phase formation and charge transport.<sup>3–8,12</sup> However, a major limitation on the molecular weight is the poor solubility of conjugated polymers. Here, the solubility issues of the BDT, CPDT, and DTP based polymers were studied. For comparison, the BDT and CPDT units with the same side chains (3,7-dimethyloctyl, or DMO) were polymerized with the DFBT unit, and the resulting polymers (PBDT–DFBT and PCPDT–DFBT) showed very poor solubility even with  $M_n$  less than 10 kDa. Especially for PBDT–DFBT, the oligomer precipitated out in less than 10 min during the polymerization reaction, and the fine particles cannot be dissolved in any common solvents. These results suggested that the DTP based polymers indeed have better solubility than polymers using symmetric building blocks. Meanwhile, PDTP–DFBT polymers with less bulky chains ( $n\text{-C}_8\text{H}_{17}$ , or  $n$ -octyl) were also synthesized but showed low solubility at  $M_n \sim 10$  kDa and cannot be used for solution processing. This means the two small branches (two methyl groups) on the DMO side chains are critically important to maintain certain solubility for the

DTP–DFBT based polymers. A photograph showing the mixtures of these polymers at ~2 mg/mL with *o*-dichlorobenzene (DCB) is shown in Figure 2. It can be seen that a lot

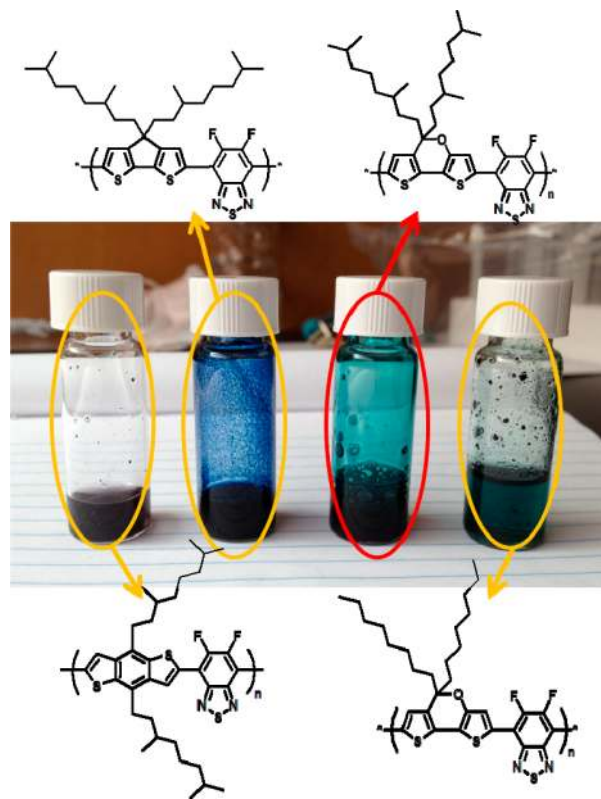


**Figure 2.** Comparison of solubility of different polymers (~2 mg/mL in DCB) at room temperature.

of particles remain in the solution for the DMO side chain based PBDT–DFBT, PCPDT–DFBT polymer, and the  $n$ -octyl chain based DTP–DFBT polymer, whereas the PDTP–DFBT with DMO chains ( $M_n = 28.5$  kDa) was fully dissolved. We attribute the better solubility of the DTP based polymer to the following possible reasons: first, the regiorandom polymer backbone is more disordered, and thus intermolecular interactions maybe weaker; second, the larger backbone curvature of the DTP–DFBT based polymer (bending angle  $\sim 120^\circ$ ) compared to BDT–DFBT (linear,  $180^\circ$ ) or CPDT–DFBT (slightly bent,  $\sim 140^\circ$ ) based polymers (see Figure S5) may lead to better solubility (for more details, see ref 13 by Müllen et al., discussing the effects of the backbone curvature on solubility and charge carrier mobility).<sup>13</sup> Preliminary X-ray diffraction study on PDTP–DFBT thin film shows no significant diffraction peak in the out-of-plane direction, which is probably due to the preference of “face on” packing orientation or the amorphous nature of the polymer. Further investigation using grazing incidence wide-angle X-ray scattering technique will be carried out to draw a clear picture on the molecular packing and thus to gain more insight into the solubility issues.

**Optical and Electrochemical Properties of the Monomers and Polymers.** The electron-donating property of the DTP unit was examined using cyclic voltammetry (CV) measurement, and the results are shown in Figure 3. The measured HOMO levels for the BDT, CPDT, and DTP units are  $-5.36$ ,  $-5.26$ , and  $-5.20$  eV, respectively. These results

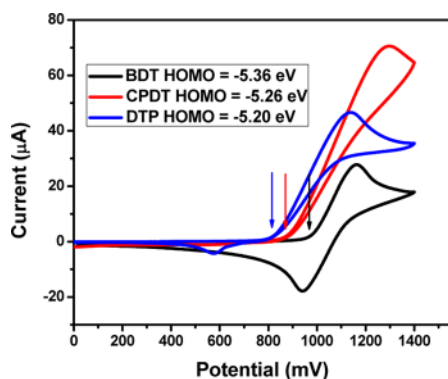


**Figure 3.** Cyclic voltammograms of BDT, CPDT, and DTP compounds with DMO side chains in  $\text{CH}_3\text{CN}$  (10 mg/mL).

were further confirmed by density functional theory calculation, and the calculated values for them are  $-5.22$ ,  $-5.17$ , and  $-5.06$  eV, respectively (Figure S6). Both experimental and theoretical results indicated that the DTP unit has a higher HOMO level than BDT and CPDT unit. The significantly higher HOMO level of the DTP unit can be attributed to the strongly electron-donating oxygen atom in the pyran ring. Therefore, the electron donating strength of these units follows the trend  $\text{BDT} < \text{CPDT} < \text{DTP}$ . In this way the copolymers based on the DTP and DFBT unit should have lowest energy bandgap compared to the BDT and CPDT based copolymers.

Figure 4 shows the ultraviolet/visible (UV/vis) absorption spectra of the PDTP–DFBT in dilute solution (CB) and thin

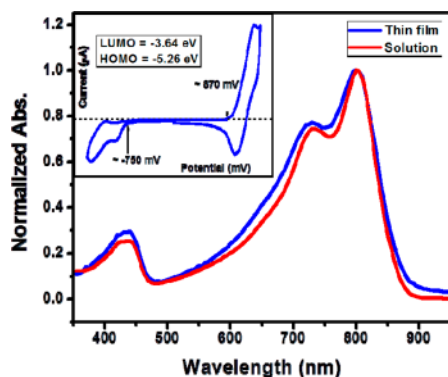


**Figure 4.** Absorption spectra of PDTP–DFBT in chlorobenzene ( $\sim 0.1$  mg/mL) and thin film casted from chlorobenzene; cyclic voltammetry of PDTP–DFBT thin film (inset).

film, and the cyclic voltammetry of the polymer film is shown in the inset. Compared to the absorption in solution, very slight broadening of the spectrum for the solid state is observed. The polymer has a main absorption range from  $\sim 600$  to  $\sim 900$  nm, and the absorption onset is located at  $\sim 890$  nm. The optical bandgap of PDTP–DFBT is calculated to be  $1.38$  eV. The bandgap is indeed lower than the BDT or CPDT based copolymers.<sup>4c,6,8</sup> Such a small energy bandgap is attributed to the intramolecular charge transfer between the strongly electron-donating DTP unit and strongly electron-withdrawing DFBT unit.<sup>2</sup> The HOMO and LUMO energy levels of PDTP–DFBT were measured to be  $-5.26/-3.64$  eV, and the electrochemical bandgap is around  $1.6$  eV. The LUMO level of PDTP–DFBT is more than  $0.3$  eV higher than PCBM ( $-4.0$

eV measured by our system), and it is high enough for efficient charge separation at the donor–acceptor interface.<sup>1,2</sup>

**BHJ Solar Cell Performance.** BHJ solar cell performance of PDTP–DFBT was investigated by making devices with the regular structure of ITO/PEDOT:PSS (30 nm)/PDTP–DFBT:PC<sub>71</sub>BM (100 nm)/Ca/Al under AM1.5G illumination ( $100 \text{ mW}/\text{cm}^2$ ). Different batches of PDTP–DFBT with various  $M_n$  were synthesized and examined in BHJ solar cell devices to demonstrate the importance of molecular weight control on the OPV performance. The polymer was spin-coated onto the PEDOT:PSS-coated indium-doped tin oxide (ITO) glass substrate from DCB solution, followed by the evaporation of Ca/Al as top electrode. The optimized polymer:PC<sub>71</sub>BM ratio was found to be 1:2 by weight (see Figure S7). Typical current density–voltage ( $J$ – $V$ ) curves are shown in Figure 5a,

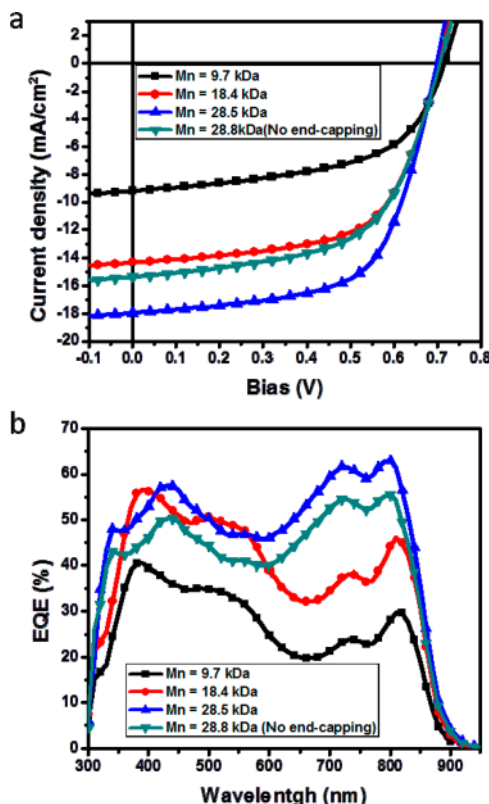


**Figure 5.** (a) Current density–voltage characteristics of PDTP–DFBT/PC<sub>71</sub>BM BHJ solar cells under AM1.5G illumination ( $100 \text{ mW}/\text{cm}^2$ ). (b) EQEs of the corresponding devices.

and the corresponding EQE curves are presented in Figure 5b; the results are summarized in Table 1. Under the best conditions, the highest/average PCE was measured to be  $8.0/7.8\%$  with a  $V_{\text{OC}}$  of  $0.698$  V, a  $J_{\text{SC}}$  of  $18.0 \text{ mA}/\text{cm}^2$ , and a FF of

**Table 1.** Photovoltaic Properties of Single-Layer BHJ Solar Cells Based on PDTP–DFBT:PC<sub>71</sub>BM

$M_n$ (kDa)	$V_{\text{OC}}$ (V)	$J_{\text{SC}}$ ( $\text{mA}/\text{cm}^2$ )	FF (%)	PCE <sub>max/aver</sub> (%)
9.7	0.710	9.0	59.8	3.8/3.5
18.4	0.706	14.5	61.8	6.3/6.1
28.5	0.698	18.0	63.4	8.0/7.8
28.8 <sup>a</sup>	0.702	15.8	60.6	6.8/6.5

<sup>a</sup>Without end-capping and washing.

63.4% for the high molecular weight PDTP–DFBT. As shown in Table 1, it is clear that lowering the molecular weight leads to lower performance: as the  $M_n$  decreased from 28.5K to 18.4K to 9.7K, the maximum PCE dropped from 8.0% to 6.3% to 3.8%, mainly due to the lower  $J_{SC}$ . These results are in accordance with previously reported ones.<sup>7e</sup> To examine the effects of tin removal, high- $M_n$  PDTP–DFBT without end-capping and washing was synthesized and tested. As shown in Table 1, about 10% lower  $J_{SC}$  (15.8 mA/cm<sup>2</sup>) and FF (60.6%) were obtained compared to the one with end-capping and washing at similar  $M_n$ , which demonstrates the effectiveness of the tin-removal procedure. The technical details disclosed here should benefit the community greatly and allow them to repeat our results and make even better materials in the future. From the external quantum efficiency (EQE) results (Figure 5b), a broad coverage from 300 to 900 nm is clearly seen. Also, the average values are around 60% within the whole region. The high hole mobility of PDTP–DFBT (up to  $3 \times 10^{-3}$  cm<sup>2</sup> V<sup>-1</sup> s<sup>-1</sup>) determined by the space charge limited current model and the favorable morphology of the blend film both contribute to its high photovoltaic performance. To examine the morphology of the polymer:PC<sub>71</sub>BM blend films at different molecular weight, transmission electron microscopy (TEM) images were taken and shown in Figure 6. The dark and light regions represent

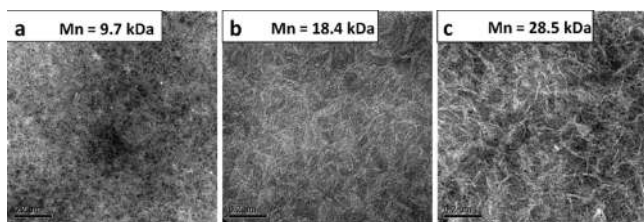


**Figure 6.** TEM images of PDTP–DFBT:PC<sub>71</sub>BM (w/w = 1:2) blend film casted from DCB. The scale bar is 200 nm.

fullerene and polymer domains, respectively. It is clear that as  $M_n$  increases, stronger phase separation and larger fibril features can be observed. This type of morphology is expected to improve charge separation and transport.<sup>3b,8a</sup> These results are consistent with the superior performance of the high molecular weight PDTP–DFBT compared to the low molecular weight ones.

For comparison, a soluble PCPDT–DFBT using two DMO side chains at low  $M_n$  (~6 kDa) was synthesized and tested (PBDT–DFBT was not tested due to the extremely poor solubility). However, the photovoltaic performance was rather low with PCE = 3.3% ( $V_{OC}$  = 0.82 V,  $J_{SC}$  = 7.6 mA/cm<sup>2</sup>, FF = 0.52; see Figure S8 for the  $J$ – $V$  curve), which is possibly due to the relatively low hole mobility ( $4 \times 10^{-4}$  cm<sup>2</sup> V<sup>-1</sup> s<sup>-1</sup>) and poor morphology (Figure S9). Higher molecular weight PCPDT–DFBT with DMO chains showed limited solubility in common solvents and cannot be used for solution processing. By using bulkier 2-ethylhexyl side chains to increase solubility, we have demonstrated 5.6% PCE for the high molecular weight PCPDT–DFBT based devices.<sup>4c</sup> Nevertheless, the  $J_{SC}$  and FF are still significantly lower than PDTP–DFBT based devices due to lower charge carrier mobility and nonideal thin film morphology. These results demonstrate the DTP unit can lower the bandgap and increase the solubility of the copolymers significantly, and thus excellent photovoltaic performance can be achieved by increasing the molecular weight.

## CONCLUSION

In summary, we have demonstrated the design and synthesis of 5H-dithieno[3,2-b:2',3'-d]pyran as an asymmetric strongly electron-rich building block for photovoltaic polymers. The asymmetric DTP unit was constructed via Baeyer–Villiger oxidation by sodium perborate monohydrate. A LBG polymer PDTP–DFBT based on alternating DTP and DFBT units was synthesized. The strong electron-donating property of the DTP unit led to a low energy bandgap of 1.38 eV. High molecular weight PDTP–DFBT using two DMO side chains was obtained, which enables good charge transport properties and favorable thin film morphology when blended with PC<sub>71</sub>BM. BHJ solar cell devices based on PDTP–DFBT showed PCE as high as 8.0% with photoresponse up to 900 nm. This is the highest efficiency reported so far for a polymer with a bandgap less than 1.5 eV. This preliminary study demonstrates DTP is a promising building block for high-performance polymer solar cell materials. More importantly, the use of asymmetric units may benefit future materials design toward even higher efficiencies. Further investigation of regioregular PDTP–DFBT as well as other copolymers based on the DTP unit should be carried out.

## ASSOCIATED CONTENT

### Supporting Information

Experimental procedures for materials characterization, and device fabrication, NMR spectra of monomers and polymers, DFT calculations, Figure S1–S9. This material is available free of charge via the Internet at <http://pubs.acs.org>.

## AUTHOR INFORMATION

### Corresponding Author

\*E-mail: yoshimurak2@sc.sumitomo-chem.co.jp (K.Y.); yangy@ucla.edu (Y.Y.).

### Notes

The authors declare no competing financial interest.

## ACKNOWLEDGMENTS

This work was financially supported by Air Force Office of Scientific Research (FA9550-09-1-0610) and Sumitomo Chemical Co., Ltd. We thank Dr. Gang Li, Dr. Jingbi You, and Ms. Chia-Jung Hsu for the helpful discussion and TGA/XRF measurement, respectively. We thank Enlitech Co., Ltd., for providing EQE measurement equipments.

## REFERENCES

- (1) (a) Yu, G.; Gao, J.; Hummelen, J. C.; Wudl, F.; Heeger, A. J. *Science* **1995**, *270*, 1789. (b) Li, G.; Shrotriya, V.; Huang, J. S.; Yao, Y.; Moriarty, T.; Emery, K.; Yang, Y. *Nat. Mater.* **2005**, *4*, 864. (c) Krebs, F. C. *Sol. Energy Mater. Sol. Cells* **2009**, *93*, 394. (d) Brabec, J.; Sariciftci, N. S.; Hummelen, J. C. *Adv. Funct. Mater.* **2011**, *11*, 15. (e) Li, G.; Zhu, R.; Yang, Y. *Nat. Photonics* **2012**, *6*, 153. (f) Chen, C.-C.; Dou, L. T.; Zhu, R.; Chung, C.-H.; Song, T.-B.; Zheng, Y. B.; Hawks, S.; Li, G.; Weiss, P. S.; Yang, Y. *ACS Nano* **2012**, *6*, 7185.
- (2) (a) Thompson, B. C.; Frechet, J. M. J. *Angew. Chem., Int. Ed.* **2008**, *47*, 58. (b) Cheng, Y. J.; Yang, S. H.; Hsu, C. S. *Chem. Rev.* **2009**, *109*, 5868. (c) Boudreault, P. L. T.; Najari, A.; Leclerc, M. *Chem. Mater.* **2011**, *23*, 456. (d) Beaujuge, P. M.; Frechet, J. M. J. *J. Am. Chem. Soc.* **2011**, *133*, 20009. (e) Li, Y. F. *Acc. Chem. Res.* **2012**, *45*, 723.
- (3) (a) Chen, H.-Y.; Hou, J. H.; Zhang, S. Q.; Liang, Y. Y.; Yang, G. W.; Yang, Y.; Yu, L. P.; Wu, Y.; Li, G. *Nat. Photonics* **2009**, *3*, 649–653. (b) Liang, Y. Y.; Xu, Z.; Xia, J.; Tsai, S. T.; Wu, Y.; Li, G.; Ray, C.; Yu,



- L. P. *Adv. Mater.* **2010**, *22*, E135. (c) He, Z. C.; Zhong, C. M.; Su, S. J.; Xu, M.; Wu, H. B.; Cao, Y. *Nat. Photonics* **2012**, *6*, 591. (d) Amb, C. M.; Chen, S.; Graham, K. R.; Subbiah, J.; Small, C. E.; So, F.; Reynolds, J. R. *J. Am. Chem. Soc.* **2011**, *133*, 10062. (e) Chu, T. Y.; Lu, J. P.; Beaupre, S.; Zhang, Y. G.; Pouliot, J. R.; Wakim, S.; Zhou, J. Y.; Leclerc, M.; Li, Z.; Ding, J. F.; Tao, Y. *J. Am. Chem. Soc.* **2011**, *133*, 4250. (f) Huo, L. J.; Zhang, S. Q.; Guo, X.; Xu, F.; Li, Y. F.; Hou, J. H. *Angew. Chem., Int. Ed.* **2011**, *50*, 9697. (g) You, J. B.; Chen, C.-C.; Dou, L. T.; Murase, S.; Duan, H.-S.; Hawks, S.; Xu, T.; Son, H. J.; Yu, L. P.; Li, G.; Yang, Y. *Adv. Mater.* **2012**, *24*, 5267. (h) Zhou, J. Y.; Wan, X. J.; Liu, Y. S.; Zuo, Y.; Li, Z.; He, G. G.; Long, G. K.; Ni, W.; Li, C. X.; Su, X. C.; Chen, Y. S. *J. Am. Chem. Soc.* **2012**, *134*, 16345. (i) Xu, Y.-X.; Chueh, C.-C.; Yip, H.-L.; Ding, F.-Z.; Li, Y.-X.; Li, C.-Z.; Li, X.; Chen, W.-C.; Jen, A. K.-Y. *Adv. Mater.* **2012**, *24*, 6356.
- (4) (a) Dou, L. T.; You, J. B.; Yang, J.; Chen, C.-C.; He, Y. J.; Murase, S.; Moriarty, T.; Emery, K.; Li, G.; Yang, Y. *Nat. Photonics* **2012**, *6*, 180. (b) Dou, L. T.; Gao, J.; Richard, E.; You, J. B.; Chen, C.-C.; Cha, K. C.; He, Y. J.; Li, G.; Yang, Y. *J. Am. Chem. Soc.* **2012**, *134*, 10071. (c) You, J. B.; Dou, L. T.; Yoshimura, K.; Kato, T.; Ohya, K.; Moriarty, T.; Emery, K.; Chen, C.-C.; Gao, J.; Li, G.; Yang, Y. *Nat. Commun.* **2013**, *4*, 1446. (d) Dou, L. T.; Chang, W.-H.; Gao, J.; You, J. B.; Yang, Y. *Adv. Mater.* **2013**, *25*, 825. (e) Li, W. W.; Furlan, A.; Hendricks, K. H.; Wienk, M. M.; Janssen, R. A. J. *J. Am. Chem. Soc.* **2013**, *135*, 5529.
- (5) (a) Blouin, N.; Michaud, A.; Leclerc, M. *Adv. Mater.* **2007**, *19*, 2295. (b) Park, S. H.; Roy, A.; Beaupre, S.; Cho, S.; Coates, N.; Moon, J. S.; Moses, D.; Leclerc, M.; Lee, K.; Heeger, A. J. *Nat. Photonics* **2009**, *3*, 297.
- (6) (a) Hou, J.; Park, M.-H.; Zhang, S.; Yao, Y.; Chen, L.-M.; Li, J.-H.; Yang, Y. *Macromolecules* **2008**, *41*, 6012. (b) Liang, Y.; Wu, Y.; Feng, D.; Tsai, S.-T.; Son, H.-J.; Li, G.; Yu, L. *J. Am. Chem. Soc.* **2009**, *131*, 56. (c) Liang, Y.; Feng, D.; Wu, Y.; Tsai, S.-T.; Li, G.; Ray, C.; Yu, L. *J. Am. Chem. Soc.* **2009**, *131*, 7792. (d) Zou, Y.; Najari, A.; Berrouard, P.; Beaupre, S.; Reda Aich, B.; Tao, Y.; Leclerc, M. *J. Am. Chem. Soc.* **2010**, *132*, 5330. (e) Zhang, Y.; Hau, S. K.; Yip, H.-L.; Sun, Y.; Acton, O.; Jen, A. K. Y. *Chem. Mater.* **2010**, *22*, 2696. (f) Piliago, C.; Holcombe, T. W.; Douglas, J. D.; Woo, C. H.; Beaujuge, P. M.; Frechet, J. M. J. *J. Am. Chem. Soc.* **2010**, *132*, 7595.
- (7) (a) Hou, J. H.; Chen, H. Y.; Zhang, S. Q.; Li, G.; Yang, Y. *J. Am. Chem. Soc.* **2008**, *130*, 16144. (b) Zhang, M.; Fan, H.; Guo, X.; He, Y.; Zhang, Z.; Min, J.; Zhang, J.; Zhan, X.; Li, Y. *Macromolecules* **2010**, *43*, 5706. (c) Zhang, Z.; Min, J.; Zhang, S.; Zhang, J.; Li, Y. *Chem. Commun.* **2011**, *47*, 9474. (d) Subramaniam, S.; Xin, H.; Kim, F. S.; Shoaee, S.; Durrant, J. R.; Jenekhe, S. A. *Adv. Energy Mater.* **2011**, *1*, 854. (e) Coffin, R. C.; Peet, J.; Rogers, J.; Bazan, G. C. *Nat. Chem.* **2009**, *1*, 657.
- (8) (a) Peet, J.; Kim, J. Y.; Coates, N. E.; Ma, W. L.; Moses, D.; Heeger, A. J.; Bazan, G. C. *Nat. Mater.* **2007**, *6*, 497. (b) Zhu, Z.; Waller, D.; Gaudiana, R.; Morana, M.; Muhlbacher, D.; Scharber, M.; Brabec, C. *Macromolecules* **2007**, *40*, 1981. (c) Albrecht, S.; Janietz, S.; Schindler, W.; Frisch, J.; Kurpiers, J.; Kniepert, J.; Inal, S.; Pingel, P.; Fostiropoulos, K.; Koch, N.; Neher, D. *J. Am. Chem. Soc.* **2012**, *134*, 14932. (d) Zhang, Y.; Zou, J.; Cheuh, C.-C.; Yip, H.-L.; Jen, A. K.-Y. *Macromolecules* **2012**, *45*, 5427.
- (9) (a) Yoshimura, K.; Ohya, K. Patent WO 2011/136311 A1. (b) Yoshimura, K.; Ohya, K. Patent WO 2011/052709 A1.
- (10) Espiritu, M.; Handley, P. N.; Neumann, R. *Adv. Synth. Catal.* **2003**, *345*, 325.
- (11) Zhou, H.; Yang, L.; Stuart, A. C.; Price, S. C.; Liu, S.; You, W. *Angew. Chem., Int. Ed.* **2011**, *50*, 2995.
- (12) Jones, R. L.; Kumar, S. K.; Ho, D. L.; Briber, R. M.; Russell, T. P. *Nature* **1999**, *400*, 146.
- (13) Rieger, R.; Beckmann, D.; Mavrinskiy, A.; Kastler, M.; Müllen, K. *Chem. Mater.* **2010**, *22*, 5314.